Atmos. Chem. Phys., 14, 8089–8103, 2014
www.atmos-chem-phys.net/14/8089/2014/
doi:10.5194/acp-14-8089-2014

Atmospheric Chemistry and Physics
Open Access

Seasonal and elevational variations of black carbon and dust in snow and ice in the Solu-Khumbu, Nepal and estimated radiative forcings

S. Kaspari[1], T. H. Painter[2], M. Gysel[3], S. M. Skiles[4,5], and M. Schwikowski[6]

[1]Department of Geological Sciences, Central Washington University, Ellensburg, Washington, USA
[2]Jet Propulsion Laboratory, California Institute of Technology, Pasadena, California, USA
[3]Laboratory of Atmospheric Chemistry, Paul Scherrer Institut, Villigen PSI, Switzerland
[4]Department of Geography, University of California, Los Angeles, California, USA
[5]Joint Institute for Regional Earth System Science and Engineering, University of California, Los Angeles, California, USA
[6]Laboratory of Radiochemistry and Environmental Chemistry, Paul Scherrer Institut, Villigen PSI, Switzerland

Correspondence to: S. Kaspari (kaspari@geology.cwu.edu)

Received: 12 September 2013 – Published in Atmos. Chem. Phys. Discuss.: 23 December 2013
Revised: 30 June 2014 – Accepted: 4 July 2014 – Published: 13 August 2014

Abstract. Black carbon (BC) and dust deposited on snow and glacier surfaces can reduce the surface albedo, accelerate snow and ice melt, and trigger albedo feedback. Assessing BC and dust concentrations in snow and ice in the Himalaya is of interest because this region borders large BC and dust sources, and seasonal snow and glacier ice in this region are an important source of water resources. Snow and ice samples were collected from crevasse profiles and snow pits at elevations between 5400 and 6400 m a.s.l. from Mera glacier located in the Solu-Khumbu region of Nepal during spring and fall 2009, providing the first observational data of BC concentrations in snow and ice from the southern slope of the Himalaya. The samples were measured for Fe concentrations (used as a dust proxy) via ICP-MS, total impurity content gravimetrically, and BC concentrations using a Single Particle Soot Photometer (SP2). Measured BC concentrations underestimate actual BC concentrations due to changes to the sample during storage and loss of BC particles in the ultrasonic nebulizer; thus, we correct for the underestimated BC mass. BC and Fe concentrations are substantially higher at elevations < 6000 m due to post-depositional processes including melt and sublimation and greater loading in the lower troposphere. Because the largest areal extent of snow and ice resides at elevations < 6000 m, the higher BC and dust concentrations at these elevations can reduce the snow and glacier albedo over large areas, accelerating melt, affecting glacier mass balance and water resources, and contributing to a positive climate forcing. Radiative transfer modeling constrained by measurements at 5400 m at Mera La indicates that BC concentrations in the winter–spring snow/ice horizons are sufficient to reduce albedo by 6–10 % relative to clean snow, corresponding to localized instantaneous radiative forcings of 75–120 W m^{-2}. The other bulk impurity concentrations, when treated separately as dust, reduce albedo by 40–42 % relative to clean snow and give localized instantaneous radiative forcings of 488 to 525 W m^{-2}. Adding the BC absorption to the other impurities results in additional radiative forcings of 3 W m^{-2}. The BC and Fe concentrations were used to further examine relative absorption of BC and dust. When dust concentrations are high, dust dominates absorption, snow albedo reduction, and radiative forcing, and the impact of BC may be negligible, confirming the radiative transfer modeling. When impurity concentrations are low, the absorption by BC and dust may be comparable; however, due to the low impurity concentrations, albedo reductions are small. While these results suggest that the snow albedo and radiative forcing effect of dust is considerably greater than BC, there are several sources of uncertainty. Further observational studies are needed to address the contribution of BC, dust, and colored organics to albedo reductions and snow and ice melt, and to characterize the time variation of radiative forcing.

Published by Copernicus Publications on behalf of the European Geosciences Union.

1 Introduction

Recent research has focused on assessing black carbon (BC, the strongest absorbing component of soot) concentrations in snow and ice. BC is produced by the incomplete combustion of biomass, coal and, diesel fuels. In the atmosphere, BC absorbs light and causes atmospheric heating, whereas BC deposited on snow and ice can reduce the surface albedo, accelerate snow and ice melt, and trigger albedo feedback (Flanner et al., 2009; Hansen and Nazarenko, 2004; Ramanathan and Carmichael, 2008). BC is estimated to be second only to CO_2 in its contribution to climate forcing (Ramanathan and Carmichael, 2008; Bond et al., 2013), and the effect of BC on snow albedo further contributes to climate warming (Hansen and Nazarenko, 2004). However, the degree to which BC contributes to climate warming and changes in the hydrologic cycle remains uncertain.

Assessing BC concentrations in the Himalaya and Tibetan Plateau is of particular interest because this region borders some of the largest sources of BC globally (Bond et al., 2007). Regional sources of BC include biomass burning (forest and grassland fires, burning of agricultural and crop waste), residential cooking and heating, transportation, power generation, and industry (Bond et al., 2004; Venkataraman et al., 2005, 2006). The largest climate forcing from BC in snow is estimated to occur over the Himalaya and Tibetan Plateau (Ramanathan and Carmichael, 2008; Flanner et al., 2007, 2009), and there are concerns that BC is contributing to glacier retreat in this region via atmospheric heating and albedo reduction due to BC deposition on glacier surfaces (Ramanathan and Carmichael, 2008). Glacier retreat in this region has serious consequences as snow and runoff from Himalayan glaciers are sources of major rivers in Asia and as the availability of water resources has profound effects on agriculture and human health (Barnett et al., 2005; Immerzeel et al., 2010). While glaciers in the Himalaya are retreating, it is not clear if the retreat is driven by rising temperatures or deposition of BC and other light-absorbing impurities (Bolch et al., 2012).

Prior research has begun to characterize BC concentrations in snow and ice in this region both spatially and temporally. Ming et al. (2009) analyzed snow pits for BC from glaciers in western China and reported that BC concentrations are highest in the periphery of the Tibetan Plateau and at lower elevations, likely due to the closer vicinity to sources, and melting, which concentrates the BC load. Historical records of BC concentrations in snow and ice have been produced from ice cores retrieved from mountain glaciers, with most studies reconstructing BC concentrations since the 1950s. These studies suggest that BC concentrations on the Tibetan Plateau were highest during the 1950s–1960s, during which Tibetan glaciers retreated, whereas cores from the Himalaya indicate elevated BC concentrations in recent decades (Liu et al., 2008; Ming et al., 2008; Xu et al., 2009). An ice core retrieved from the East Rongbuk Glacier on the northern slope of Mt. Everest and spanning 1860–2000 provided the first Asian ice core record of BC concentrations since pre-industrial times, and documented a threefold increase in BC concentrations from 1975–2000 relative to 1860–1975 (Kaspari et al., 2011). The differences in BC temporal trends between sites is attributed to source differences, with the Tibetan Plateau sites thought to be dominated by European BC sources, whereas modeling studies and comparisons of ice core records with historical BC emission inventories suggest that the dominant sources of BC deposited in the Himalaya are from South Asia, with lesser contributions from the Middle East (Kopacz et al., 2011; Kaspari et al., 2011; Bond et al., 2007; Xu et al., 2009).

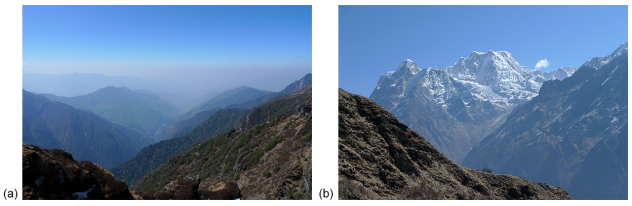

Figure 1. Photographs taken from the same location in the Inkhu Khola valley, Solu-Khumbu, Nepal at ∼4300 m. **(a)** looking south. Note the presence of the Atmospheric Brown Cloud (a combination of BC, other pollutants and dust). Picture **(b)** looking northwards towards the crest of the Himalaya (here seeing the south side of Mera Peak).

Previous BC observational work has focused on BC concentrations in snow and ice on the northern slope of the Himalaya, despite the proximity of the south slope of the Himalaya to major BC sources (Fig. 1). Conducting field research on the south slope of the Himalaya is logistically challenging, and as a result there is a paucity of in situ data. While Yasunari et al. (2010) used atmospheric data to estimate BC deposition onto glaciers on the southern slope of the Himalaya, no southern slope observational data of BC concentrations in snow/ice has been available besides the study presented herein and recent work by Ginot et al. (2013).

While recent research has largely focused on BC, dust and other light-absorbing impurities also reduce snow albedo and can be present in snow in much higher concentrations than BC (e.g., Kaspari et al., 2011; Painter et al., 2007; Takeuchi et al., 2002). Furthermore, there is evidence that dust deposition in the Himalaya may be increasing due to anthropogenic activities and increased aridity (e.g., Thompson et al., 2000; Kaspari et al., 2009), and recent remote sensing studies suggest that dust may dominate solar absorption (Gautam et al., 2013; Ming et al., 2012). However, the lack of in situ data from this region prevents evaluating the effect of BC and dust deposition on snow and ice albedo and melt. Ginot et al. (2013) analyzed a shallow ice core retrieved in 2010 from the summit of Mera Peak in the Solu-Khumbu region of Nepal for BC, dust and stable isotopes, and used the resultant record to estimate the potential impact of BC and dust

on glacier melting. While this record provided valuable information on the interannual variability of BC and dust deposition to the accumulation zone of Mera glacier, this study did not take into account that BC and dust concentrations are higher at lower elevations, affecting their melt estimates.

Herein we present BC and dust concentrations in snow and ice from the ablation and accumulation zones of Mera glacier located on the southern slope of the Himalaya in the Solu-Khumbu region of Nepal. We investigate how BC and dust concentrations vary seasonally and with elevation due to differences in deposition and post-depositional processes, and we estimate the associated changes in snow albedo and radiative forcings by BC and dust in snow.

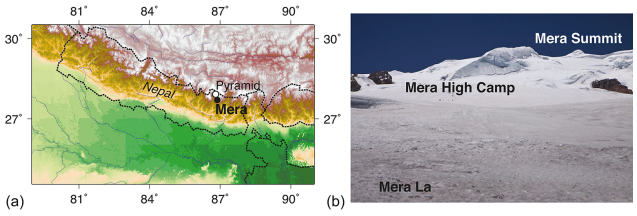

Figure 2. (a) Location of Mera Peak and Nepal Climate Observatory-Pyramid, and **(b)** Picture of Mera glacier taken during April 2009 showing the location of Mera La (5400 m a.s.l.), Mera High Camp (5800 m a.s.l.), and Mera Summit (6400 m a.s.l.). Photo taken by Jesse Cunningham.

2 Site description and methods

2.1 Site description

Mera glacier (27°43 N, 86°53 E) in the Solu-Khumbu region of Nepal was selected as the study site for this research because Mera glacier is: (1) located on the southern slope of the Himalaya; (2) a debris free glacier that has been monitored for glacier mass balance since 2007 (Wagnon et al., 2013); (3) located nearby (30 km south of) the Nepal Climate Observatory-Pyramid (NCO-P) in the Khumbu valley, Nepal (27°56 N, 86°49 E, 5079 m a.s.l.) where atmospheric BC measurements have been made since 2006; and (4) relatively accessible (5–7 days walk from Lukla airport). During the summer months the climate at this site is dominated by the Indian monsoon, with air masses originating from the Bay of Bengal. During the winter, atmospheric circulation is dominated by the westerlies. Based on NCO-P station data, more than 80 % of the precipitation falls during the summer monsoon period (June–September), with the non-monsoon months relatively dry. Mera glacier flows northwards from the summit of Mera Peak (6420 m a.s.l.) to the terminus at 4940 m a.s.l., and the equilibrium line altitude (ELA) is located at approximately 5550 m a.s.l. The monitoring of Mera glacier since 2007 indicates that the glacier is undergoing moderate mass loss (Wagnon et al., 2013).

2.2 Sample collection

To characterize BC and dust concentrations in snow and ice, snow/ice samples were collected during spring and fall 2009 at elevations between 5400 and 6400 m a.s.l. (Fig. 2). In late April 2009, samples were collected from northwest-facing crevasse profiles near Mera La (5400 m a.s.l., and below the ELA) and below Mera High Camp (5800 m a.s.l., and above the ELA). The density of the firn, particularly at Mera La, was not conducive to snow pit sampling, and the crevasse profiles enabled multiple years of firn to be sampled. Because the surface of crevasse walls can undergo sublimation and melt processes, the outer surface of the crevasse walls were removed using a mountain axe to create a fresh sampling surface, with a minimum of 10 cm of the fresh surface being removed. The crevasse wall was continuously sampled in 5–10 cm increments directly into pre-cleaned 50 mL polypropylene vials. The upper 3 m of a crevasse was sampled near Mera La, and the upper 2 m of a crevasse was sampled below Mera High Camp. At the col below Mera Peak (6400 m a.s.l.), a 54 cm snow pit was continuously sampled in 3 cm increments. In addition to the snow/firn collected from Mera glacier, nine fresh snow samples were collected by personnel at the Nepal Climate Observatory-Pyramid (NCO-P) in the Khumbu valley, Nepal (27°56 N, 86°49 E, 5079 m a.s.l.) during February–May 2009. These samples were kept frozen until transport from NCO-P. Due to the remoteness of Mera glacier, samples were not kept frozen during transport from the field to the laboratory. Thus, samples were kept stored at ambient temperature away from light until analyzed for BC and dust at the Paul Scherrer Institut in May 2009. Additionally, during early November 2009 a 30 cm snow pit was sampled at 5 cm resolution from Mera La, a 1.2 m snow pit was sampled at 3–4 cm resolution below Mera High Camp, and a 1.7 m snow pit was sampled at 3.7 cm resolution at the col below Mera Peak. These samples were stored at ambient temperature until analyzed in October 2010 at Central Washington University. Due to the longer time period between collection and chemical analysis of the samples collected during the fall of 2009, these samples are only discussed briefly.

2.3 Dust analytical methods

All samples were acidified with nitric acid to 0.5 mol L^{-1} for consistency with the methods described in Kaspari et al. (2011). Iron (Fe) concentrations were determined by inductively coupled plasma mass spectrometry (ICP-MS) and used as a dust proxy because iron oxides dominate light absorption by mineral dust. After the samples were analyzed for BC (described below in Sect. 2.4), the impurity load in five highly concentrated samples was determined gravimetrically after drying the samples at 80 °C. Herein we make the assumption that the gravimetric impurity measurement reflects dust based on the following:

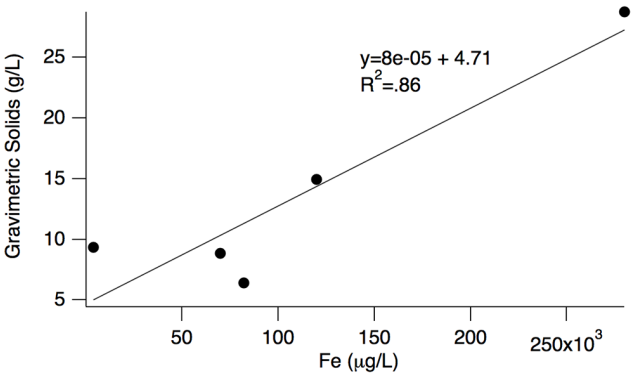

Figure 3. Fe ($\mu g\,L^{-1}$) vs. gravimetric solids ($g\,L^{-1}$) from five samples collected at Mera La.

1. The dry mass impurity is well correlated with the Fe measurements, suggesting that dust dominates the dry mass (Fig. 3).

2. Using the slope of the line in Fig. 3 and assuming a density of $1\,g\,mL^{-1}$ for the liquid samples used in the Fe measurement yields $1\,g\,Fe\,80\,g^{-1}$ of dust, indicating the dust is 1.25 % Fe, or 1.8 % Fe when scaled to hematite. This is in the expected range for Fe_2O_3 in the upper continental crust (4.4 %), granites (2 %) and sedimentary rocks (6.4 %) (Wedepohl, 1995).

3. Takeuchi et al. (2002) reported that organic material accounted for between 3.0–6.8 % of cryoconite mass on Himalayan glaciers, supporting the assumption that dust dominates the impurity mass (solids).

2.4 BC analytical method

The same samples measured via ICP-MS were analyzed for BC using a Single Particle Soot Photometer (SP2, Droplet Measurement Technologies). The SP2 uses laser-induced incandescence to measure the BC mass in individual particles (between 80–500 nm diameter in this study) quantitatively and independent of particle morphology and coatings with light scattering material (Slowik et al., 2007; Schwarz et al., 2006; Stephens et al., 2003). The SP2 detects the mass concentration of refractory BC (sometimes referred to as rBC (Petzold et al., 2013); the term BC is used here for simplicity), while other absorbing aerosol components such as brownish carbon or mineral dust are generally not detected by the SP2. Recent work indicates that the presence of dust can produce visible light signals in the SP2, which causes a small positive offset ($15\,\mu g\,L^{-1}$ BC offset for samples with very high ($50\,000\,\mu g\,L^{-1}$) dust concentrations) (Schwarz et al., 2012). In the context of this study, this offset is negligible due to the high BC concentrations reported herein, and other analytical uncertainties described below. Prior BC method comparison studies indicate that the SP2 is less affected by other light-absorbing impurities than other BC analytical methods (Schwarz et al., 2012; Torres et al., 2014; Lim et al., 2014). Additional advantages of the SP2 is that smaller sample volumes are required than other BC analytical methods, and the method does not use filters that can have filtration efficiency issues. Further details on the SP2 calibration and configuration are provided by Wendl et al. (2014) and in the auxiliary materials of Kaspari et al. (2011).

The samples were sonicated for 15 minutes just prior to analysis. During BC analyses the samples were mixed using a magnetic stirrer, nebulized using a Cetac U-5000AT+ ultrasonic nebulizer, and the resultant aerosol was introduced to the sample inlet of the SP2. Samples with measured BC concentrations exceeding $10\,\mu g\,L^{-1}$ were diluted with Milli-Q water to less than $10\,\mu g\,L^{-1}$. The monitoring of liquid sample flow rate pumped into the nebulizer, fraction of liquid sample nebulized, and nebulizer and SP2 airflow rates allows BC mass concentrations in the liquid sample to be determined. Schwarz et al. (2012) report that the SP2 combined with a Collison-type nebulizer can be used to measure BC mass concentration in snow with an estimated 60 % uncertainty (due to uncertainty in calibration results and size dependent nebulization efficiency). The BC concentrations reported herein underestimate actual concentrations, and have an uncertainty higher than 60 % due to:

1. Loss of BC particles in the Cetac U-5000AT+ ultrasonic nebulizer. Schwarz et al. (2012) tested nebulization efficiency based on particle size using polystyrene latex spheres ranging in size between 220 and 1537 nm, and reported that the Cetac nebulization efficiency was size dependent. The nebulization efficiency was 20 % or less for particles greater than 700 nm relative to particles in the 200–500 nm size range. Subsequent research at Central Washington University confirmed the results of Schwarz for the Cetac, while Wendl et al. (2014) found that for the Cetac, nebulization efficiency was greatest in the 300–400 nm size range, with decreased efficiency for smaller and larger particle sizes. Additionally, Schwarz et al. (2013) report larger mass size distributions of BC in snow than BC in the atmosphere, with the mass of BC cores larger than 600 nm accounting for 17 % or more of the BC mass based on snow samples in Colorado. Thus, a non-trivial mass of BC is not nebulized by the Cetac nebulizer, and thus not measured by the SP2. We correct for the mass of BC not nebulized based on gravimetric Aquadag standard solutions. This standard correction does not fully address the size dependent nebulization nor likely differences in the mass-size distributions of Aquadag and the snow samples. We also note that prior studies using the SP2 to measure BC concentrations in liquid samples have used other BC materials as a calibration standard, with other

standards resulting in a higher corrected BC concentration than Aquadag (Wendl et al., 2014).

2. Apparent BC losses due to changes to the sample during storage. Repeated measurements on aqueous samples stored at ambient temperature demonstrate a reduction in measured BC concentrations over time (Wendl et al., 2014). Re-measuring Aquadag standards and environmental samples stored at room temperature in polypropylene vials over an 18 day period indicated that BC losses are dependent on sample concentration. Aquadag standards that measured 7, 5, and 2 $\mu g\,L^{-1}$ BC directly after the standards were created decreased to 4, 1.8, and 0.3 $\mu g\,L^{-1}$ BC, indicating that measured concentrations after 18 days were 57, 36, and 15 % of the initially measured concentrations, respectively. An environmental snow sample that initially was measured as having a concentration of 2.4 $\mu g\,L^{-1}$ BC decreased to 0.6 $\mu g\,L^{-1}$ after 18 days, or 25 % of the initially measured concentration (Wendl et al., 2014). These results suggest that apparent BC losses are proportionally greater in low concentration samples relative to higher concentration samples. The samples from Mera glacier were analyzed 3 weeks after sample collection, so the above-mentioned BC losses may be referred to in order to estimate apparent BC losses in the Mera samples. However, complications in extrapolating the above results to the Mera samples include (1) BC concentrations in some of the Mera samples are one to two magnitudes greater than the prepared standards. BC losses in highly concentrated samples are likely proportionally lower than low concentration samples, as indicated by the above results, and (2) the Mera samples have high dust concentrations, and it is not known how the chemical composition of the sample affects apparent BC losses. Possible causes of the BC losses during storage include BC particles agglomerating above the size range in which particles are efficiently nebulized and outside of the detection range of the SP2, and/or BC adhering to the vial walls. Subsequent research has shown that acidification of samples stored in polypropylene can aid in at least partial recovery of BC losses that occur in the sample vial (Wendl et al., 2014). However, in general we advise against acidification because acidification can cause a shift towards smaller BC particles (Schwarz et al., 2012). To avoid particle losses, samples should be kept frozen from the time of collection until just prior to being measured with the SP2. As mentioned above, field logistics during this reconnaissance campaign did not make this possible in the current study.

These factors lead to uncertainties in the actual BC concentrations. Herein we report the BC concentrations as *measured* BC ($_{M}$BC), which have been corrected for the nebulizer efficiency based on the Aquadag standard solutions. The $_{M}$BC concentrations do not account for BC particles larger than those detected by our Cetac-SP2 system, nor BC particle losses that occurred during storage. Thus, the data reported herein represent lower-limit values. That the BC losses are not constant across all samples does not prevent interpretation since we focus on periods of peak signal, and $_{M}$BC concentrations span three orders of magnitude. While we predominantly focus our interpretation on relative differences in BC rather than on absolute concentrations, in Sect. 3.3 we scale the BC measurements to account for the underestimated mass to estimate absorption by BC and dust. Despite the uncertainties in the data, the results reported herein yield information that furthers our understanding of seasonal and spatial variations in BC and dust in snow and ice in the Himalaya.

3 Results and discussion

3.1 Variations of BC and dust with depth

Within the two crevasse profiles, layers of impurities were observed in the firn, interspersed with thicker low impurity layers (Fig. 4). Peak concentrations of $_{M}$BC and Fe coincide with the visible impurity layers.

The observed BC and Fe stratigraphy is largely due to seasonal variations in BC and dust deposition. Factors controlling BC and dust seasonality include variations in emissions, atmospheric transport, and precipitation (Kaspari et al., 2011; Kopacz et al., 2011). Previous research in the region has documented strong seasonality in BC and dust concentrations, with peak concentrations during the winter–spring period, and lower concentrations during the summer monsoon season. This seasonality has been observed in ice cores and snow pits (Kaspari et al., 2011; Cong et al., 2009), and atmospheric measurements from NCO-P (Marinoni et al., 2010; Bonasoni et al., 2010). Using the stable isotope record from the shallow Mera Peak ice core, Ginot et al. (2013) verified the results of these previous studies that BC concentrations peak during the winter–spring period. While the BC record in the Mera ice core showed strong seasonality, interestingly the dust seasonality was not well defined. This may be due to high background dust inputs (Ginot et al., 2013), or potentially the relatively large dust particle size analyzed (1.0 to 30 µm).

In this region of the Himalaya, the majority of precipitation occurs during the summer monsoon season, whereas the winter–spring period is drier (Wagnon et al., 2013). Summer monsoonal precipitation results in the wet deposition of BC and dust from the atmosphere during transport from emission sources to the study site, and thus lower atmospheric particle concentrations in the Himalaya during summer. The higher summer monsoonal precipitation rate relative to winter also acts to dilute the concentration of impurities distributed across the snow column. Thus, lower atmospheric

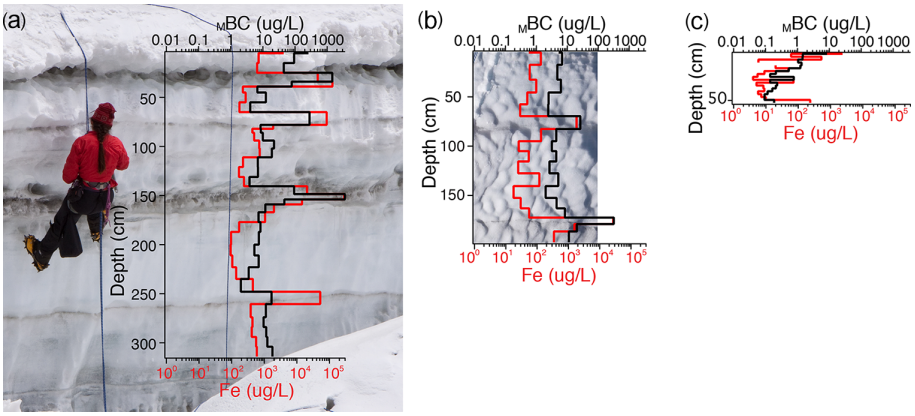

Figure 4. $_{M}$BC and Fe (used as a dust proxy) concentrations from Mera glacier crevasse profiles and snow pits from **(a)** Mera La (5400 m a.s.l.), **(b)** below Mera High Camp (5800 m a.s.l.), and **(c)** from a snow pit near the summit of Mera Peak (6400 m a.s.l.).

concentrations and higher snow accumulation keep impurity concentrations lower in summer snow and ice layers.

During the drier winter–spring months, the residence time of BC and other aerosols is longer and observed atmospheric concentrations are higher, particularly during the spring pre-monsoon season. This is the case at NCO-P, where the higher pre-monsoon atmospheric concentrations are attributed to higher vertical mixing layer heights and strong daytime up-valley winds that transport pollutants from low elevation regions (Bonasoni et al., 2010). If atmospheric aerosol concentrations are relatively higher at the study site during the winter–spring period, higher deposition of impurities on the glacier surface via dry deposition would occur at this time. Furthermore, because there is less wet removal that occurs during transport from emission sources during the drier winter–spring, there may be greater wet deposition of BC and dust at the study site when localized precipitation does occur. However, there are no atmospheric observations at elevations higher than NCO-P in the region, thus it is not known if the pre-monsoon vertically mixed layer extends to altitudes as high as the study area.

Based on the above information, for the crevasse profile sampled near Mera High Camp (5800 m a.s.l.) we conclude that the higher concentration layers are from BC and dust deposited during the winter–spring period, whereas the thicker but lower concentration layers are from snowfall during the summer monsoon. This is supported by $_{M}$BC from the snow pits sampled during November 2009, which are representative of snowfall from the summer monsoon season. $_{M}$BC from the monsoon snowfall at all three sites was $\leq 1\,\mu g\,L^{-1}$ (with the exception of two samples at Mera La that measured 3 and $7\,\mu g\,L^{-1}$), consistent with the thicker low $_{M}$BC layers observed near Mera High Camp. Additionally, glacier monitoring indicates positive mass balance at this elevation on Mera glacier (Wagnon et al., 2013), demonstrating that the snow is preserved.

The crevasse profile sampled at Mera La is located below the ELA, thus we cannot attribute the variations in BC and Fe in this profile only to seasonal variations. Rather, the BC and Fe likely became melt concentrated, potentially resulting in multiple years of impurities coalescing into individual layers. Glacier monitoring extends back only to 2007, with mass balance negative at Mera La during these years. The low impurity layers in the crevasse profile at Mera La could potentially result from (1) years of strong positive mass balance when summer monsoon snow was preserved or (2) BC flushed through the snowpack and accumulated above superimposed ice layers as observed by Xu et al. (2012) on a Tian Shan glacier.

3.2 Elevational variations of BC and dust

$_{M}$BC and Fe from the snow pit and crevasse profiles collected during spring 2009 are lower at the high elevation site, and increase with decreasing elevation (Table 1, Fig. 4). The difference in $_{M}$BC and Fe with elevation is apparent in the background, average, and maximum values. This elevation gradient is likely due to greater BC and dust deposition at lower elevations because of higher atmospheric concentrations in the troposphere and/or post-depositional processes leading to enrichment of impurities.

$_{M}$BC in fresh snowfall sampled at NCO-P (5079 m a.s.l.) in the Khumbu valley during winter–spring 2009 ranged between 3–$23\,\mu g\,L^{-1}$. This is considerably lower than $_{M}$BC in the impurity layers in the crevasse profiles, suggesting that the impurities observed in the crevasse profiles result from dry deposition, and/or post-depositional processes. Snowmelt and concentration of impurities are driven by energy absorption of the impurities in snow (referred to as the "direct effect"), and by enhanced absorption by larger snow grain size due to accelerated grain growth from the direct effect (referred to as the first indirect effect) (Painter et al., 2007). These effects cause snow metamorphism that

Table 1. $_{M}$BC and Fe in snow and ice samples from Mera glacier and a Mt. Everest ice core.

		Spring			
		Mera La	Mera High Camp	Mera Col	Everest Ice Core*
	elevation (m)	5400	5800	6400	6518
	n	34	18	18	496
$_{M}$BC	max	3535.0	318.9	8.4	75.3
	average	180.0	24.4	1.0	1.5
	median	12.1	4.9	0.2	0.5
Fe	max	283 040.0	27 096.0	2357.2	2313.3
	average	18 674.8	1760.1	199.1	104.3
	median	525.0	56.8	9.0	28.8

* Based on high resolution data 1975–2002 from Kaspari et al. (2011); BC concentrations have been corrected based on Aquadag standards.

can cause impurities in the snowpack to coalesce into a single layer, as observed in annual layers in the crevasse profiles. The coalescence of impurities into a single layer is likely greater at lower elevations due to greater energy fluxes and greater direct and first indirect effects of BC. Previous studies have documented concentration of impurities at the glacier surface due to mechanical trapping during conditions of melt or sublimation, with conditions of strong melt resulting in flushing of particles to deeper in the snowpack (Xu et al., 2012; Conway et al., 1996). These processes likely occur during the winter–spring period, and lessen during the summer monsoon season when impurity concentrations are low, accumulation is higher, and the snow direct and first indirect effects are minimized, despite greater incoming solar radiation.

3.3 Albedo reductions due to BC and dust and radiative forcing implications

Light-absorbing impurities in snow and ice can reduce the surface albedo (largely in the visible wavelengths, but out to 1.1 µm), interacting with more than half of the at-surface irradiance (the direct effect) (Painter, 2011; Singh et al., 2010; Painter et al., 2012). This reduction in albedo heats the snowpack by conducting energy from the heated impurities to snow grains, in turn accelerating snow metamorphism, which leads to coarser grains and further reduces snow albedo (the first feedback). These forcings warm the snow earlier and lead to an earlier and more rapid melt. The earlier emergence of glacier ice then markedly increases net energy fluxes and ablation.

Factors that affect the impurity-induced albedo reduction include snow grain size, solar zenith angle, snow depth, impurity concentration, the impurity ice/mixing state, particle morphology, and the presence of other absorbing impurities and liquid water (Wiscombe and Warren, 1980; Warren and Wiscombe, 1985; Hansen and Nazarenko, 2004). Previous model, laboratory, and observational studies have estimated the albedo reduction due to BC (Warren and Wiscombe, 1980, 1985; Grenfell et al., 1981, 1994; Hadley and Kirchstetter, 2012; Jacobson, 2004; Brandt et al., 2011; Flanner et al., 2007). Albedo reduction by impurities is greater for old snow relative to new snow, and for internally mixed BC (BC is located in the ice grain) relative to externally mixed BC (BC is separated from the ice particle) (Warren and Wiscombe, 1985; Hansen and Nazarenko, 2004).

Light-absorbing impurities besides BC that can cause albedo reductions include dust and light-absorbing carbon (colored organics) from biomass burning, humic-like substances, snow algae, and bacteria (Andreae and Gelencser, 2006; Takeuchi, 2002; Painter et al., 2007). Albedo reductions from BC will be less in the presence of other light-absorbing impurities because the other impurities capture some of the solar radiation that the BC would receive in the absence of other impurities (Kaspari et al., 2011). This is particularly relevant for glaciers in this region where the presence of other impurities can be high.

Because we did not measure spectral snow albedo at the sample sites, we must infer spectral albedo and light-absorbing impurity radiative forcing in snow from modeling constrained by the in situ measurements of $_{M}$BC and dust concentrations from Mera La, where measured concentrations were highest. Here we treat the gravimetrically determined total impurity load as dust as described in Sect. 2.3. However, a small portion of the dry mass may also consist of organic material, as Takeuchi et al. (2002) reported that organic material accounted for between 3.0–6.8 % of cryoconite mass on Himalayan glaciers. The surface concentrated layer with 258 µg L^{-1} $_{M}$BC and 9.3 g L^{-1} dust highlights the potential instantaneous radiative forcings due to $_{M}$BC and dust at Mera La. The maximum concentrations of $_{M}$BC (3535 µg L^{-1}) and gravimetric dust (28.7 g L^{-1} dust) were sampled at 154 cm depth. However, we do not estimate the spectral albedo for this layer since it may represent

convergence of multiple years of impurities and may not have resided at the glacier surface.

We estimated the Mera La spectral snow albedo using the Snow, Ice, and Aerosol Radiative (SNICAR) model (Flanner and Zender, 2006), constrained by the surface $_{\mathrm{M}}$BC and dust concentrations and using a solar zenith angle of 5° at solar noon. In order to span the range of forcings with varying grain sizes, we use snow optical grain radii of 350 and 750 µm. This span of grain sizes has been found in the presence of heavy impurity concentration loading in the Colorado River basin (Painter et al., 2013). The smaller grain sizes are coincident with the highest concentrations when snowmelt percolation causes grains to grow at depths several centimeters into the pack, leaving smaller grain sizes at the surface to be detected by remote sensing. The mass absorption coefficient (MAC) of BC is not exactly known, so we also span the range of MAC from 5.9 $\mathrm{m^2\,g^{-1}}$ to 7.5 $\mathrm{m^2\,g^{-1}}$. The BC MAC of 5.9 $\mathrm{m^2\,g^{-1}}$ is based on the theoretical MAC values calculated from Mie scattering theory for 460 nm light and BC with an index of refraction of ($n = (2.26, -1.26)$) (Schwarz et al., 2013) and the measured mass size distribution of BC volume-equivalent particle diameters (80–500 nm) from snow samples measured at Mera La, whereas the BC MAC of 7.5 $\mathrm{m^2\,g^{-1}}$ is based on values reported in the literature (Bond and Bergstrom, 2006; Chang and Charalampopoulos, 1990). Snow density is assumed to be 600 $\mathrm{kg\,m^{-3}}$, however model runs with lower snow density did not alter the results. Further information on the input fields used in SNICAR are reported in Table 2. Because $_{\mathrm{M}}$BC concentrations are lower-limit values (Sect. 2.4), we also model the spectral albedo and radiative forcings using scenarios $_{\mathrm{M}}\mathrm{BC}\times 2$ and $_{\mathrm{M}}\mathrm{BC}\times 5$ to bracket the potential upper range of BC in the surface layer.

We estimate the clear-sky spectral irradiance for wavelength range 0.305 to 4.995 µm at 0.010 µm intervals on 1 June 2009 for 5400 m elevation at solar noon using the Santa Barbara DISORT Atmospheric Radiative Transfer model (SBDART) (Ricchiazzi et al., 1998). The spectral ratios of reflected flux and irradiance give the spectral albedo and the integral of these albedos weighted by the spectral irradiance spectrum and divided by the sum of irradiance across the spectrum gives the broadband albedo:

$$\alpha = \frac{\sum_{\lambda=0.305\,\mu\mathrm{m}}^{4.995\,\mu\mathrm{m}} E(\lambda;\theta_0)\cdot\alpha_{\mathrm{sfc}}^{\mathrm{laisi}}(r;\lambda)\Delta\lambda_\lambda}{\sum_{\lambda=0.305\,\mu\mathrm{m}}^{4.995\,\mu\mathrm{m}} E(\lambda;\theta_0)\Delta\lambda_\lambda}, \quad (1)$$

where $\alpha_{\mathrm{sfc}}^{\mathrm{laisi}}$ is the modeled snow spectral albedo with BC and/or dust, E is the spectral irradiance, r is the snow optical grain size, λ is wavelength (µm), and θ_0 is the solar zenith angle for irradiance, in this case 5° at solar noon.

The convolution of the differences in spectral albedo from the clean snow spectrum with the spectral irradiance gives an estimate of the direct radiative forcing by the light-absorbing impurities (Painter et al., 2013).

$$\mathrm{RF} = \sum_{\lambda=0.305\,\mu\mathrm{m}}^{4.995\,\mu\mathrm{m}} E(\theta_0;\lambda)\cdot(\alpha_{\mathrm{sfc}}^{\mathrm{clean}}(\lambda;r) - \alpha_{\mathrm{sfc}}^{\mathrm{laisi}}(\lambda;r))\Delta\lambda, \quad (2)$$

where $\alpha_{\mathrm{sfc}}^{\mathrm{clean}}$ is the modeled clean snow spectral albedo.

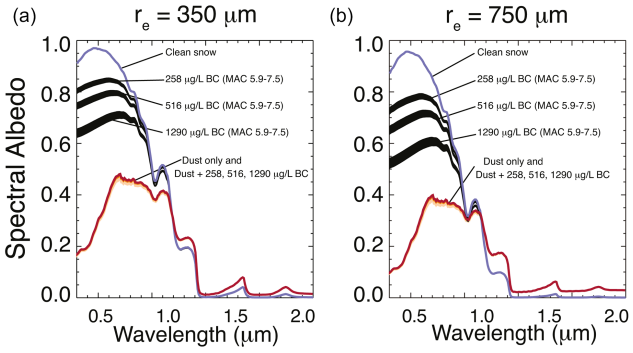

Figure 5. Modeled spectral snow albedos for the surface layer at Mera La based on dust= 9.3 g/L, $_{\mathrm{M}}$BC= 258 $\mu\mathrm{g\,L^{-1}}$, $_{\mathrm{M}}\mathrm{BC}\times 2 = 516\ \mu\mathrm{g\,L^{-1}}$, $_{\mathrm{M}}\mathrm{BC}\times 5 = 1290\ \mu\mathrm{g\,L^{-1}}$ with the MAC of BC ranging between 5.9–7.5 $\mathrm{m^2\,g^{-1}}$, and assuming snow optical grain radius of **(a)** 350 µm and **(b)** 750 µm.

The following results are based on measured BC and dust concentrations in the surface snow at Mera La. Clean snow albedos for the 350 and 750 µm grain radii particles for this solar zenith angle are 0.72 and 0.67, respectively (Table 3, Fig. 5). If BC (258 $\mu\mathrm{g\,L^{-1}}$) was the only impurity in the snowpack, the broadband albedos for the 350 and 750 µm grain radii would be 0.65–0.66 and 0.57–0.59, respectively, with associated instantaneous radiative forcings of 75–87 $\mathrm{W\,m^{-2}}$ and 104–120 $\mathrm{W\,m^{-2}}$. These forcings are based on $_{\mathrm{M}}$BC, so actual albedo reductions and radiative forcings may be larger, as indicated by the $_{\mathrm{M}}\mathrm{BC}\times 2$ and $_{\mathrm{M}}\mathrm{BC}\times 5$ scenarios (Table 3, Fig. 5). However, dust was mixed in at much larger concentrations with the BC. If dust was the only impurity in the snowpack, the broadband snow albedos for the 350 and 750 µm snow grain radii would be 0.32 and 0.25, respectively, with associated instantaneous radiative forcings of 488 and 525 $\mathrm{W\,m^{-2}}$. If BC and dust are mixed, the snow albedos are slightly changed from those for the large dust concentrations (< 0.01) and the radiative forcings only increase by 2–3 $\mathrm{W\,m^{-2}}$ over those for dust-only for the $_{\mathrm{M}}$BC scenario, and 10–11 $\mathrm{W\,m^{-2}}$ for the $_{\mathrm{M}}\mathrm{BC}\times 5$ scenario.

The optical properties of the BC and dust come from general libraries and not this specific region, and therefore the modeling of radiative forcings are relatively uncertain. Additionally, the proportion of dust that originates from localized, regional, or long-range sources has not been constrained nor is the contribution of dust from natural as opposed to anthropogenic sources well known. However, ice core records indicate that dust deposition has increased in this region (Thompson et al., 2000; Kaspari et al., 2009). Nevertheless, these

Table 2. Input field values used to estimate spectral snow albedo in SNICAR.

Grain radii	350 and 750 µm
Surface layer thickness	0.02 m
Lower layer thickness	9.98 m
Surface layer snow density	600 kg m^{-3}
Lower layer snow density	600 kg m^{-3}
Surface layer BC concentration	258 µg L^{-1}, 516 µg L^{-1}, and 1290 µg L^{-1}
Lower layer BC concentration	5 µg L^{-1}
Surface layer dust concentration (when used)	9.3 g L^{-1}
Dust size distribution	the SNICAR model's four bins that cover the size distribution in Painter et al. (2007), Lawrence et al. (2010).

Table 3. SNICAR modeled broadband snow albedo and SBDART modeled radiative forcing (W m^{-2}) based on BC and dust concentrations in the surface layer at Mera La, and assumed BC MAC and snow grain size. BC = 258 µg L^{-1} is based on $_{M}$BC, whereas BC = 516 µg L^{-1} and 1290 µg L^{-1} are $_{M}$BC × 2 and $_{M}$BC × 5 scenarios used to bracket the plausible upper range in BC concentrations at the site.

BC (ug L^{-1})	Dust (g L^{-1})	BC MAC m^2 g^{-1}	Grain Size (µm)	Broadband Snow Albedo	Radiative Forcing (W m^{-2})
0	0	–	350	0.72	–
258	0	7.5	350	0.65	87
516	0	7.5	350	0.61	130
1290	0	7.5	350	0.55	212
258	0	5.9	350	0.66	75
516	0	5.9	350	0.63	114
1290	0	5.9	350	0.57	188
0	9.3	–	350	0.32	488
258	9.3	7.5	350	0.32	491
516	9.3	7.5	350	0.32	494
1290	9.3	7.5	350	0.31	502
258	9.3	5.9	350	0.32	490
516	9.3	5.9	350	0.32	492
1290	9.3	5.9	350	0.31	499
0	0	–	750	0.67	–
258	0	7.5	750	0.57	120
516	0	7.5	750	0.53	177
1290	0	7.5	750	0.44	278
258	0	5.9	750	0.59	104
516	0	5.9	750	0.54	155
1290	0	5.9	750	0.47	248
0	9.3	–	750	0.25	525
258	9.3	7.5	750	0.25	527
516	9.3	7.5	750	0.25	530
1290	9.3	7.5	750	0.24	538
258	9.3	5.9	750	0.25	527
516	9.3	5.9	750	0.25	529
1290	9.3	5.9	750	0.24	535

results give us a preliminary idea of the order of magnitude and range of uncertainty of maximum forcing by impurities at the lower elevation Mera La site. For this surface layer, the localized instantaneous radiative forcings reasonably range from the $_{M}$BC forcings of 75 to 120 W m^{-2} to the bulk dust only and $_{M}$BC + dust radiative forcings of 488–525 W m^{-2}. Using the $_{M}$BC × 5 scenario results in instantaneous radiative forcings ranging from 188 to 248 W m^{-2} to the bulk dust only and $_{M}$BC × 5 + dust radiative forcings of 499–535 W m^{-2}. We emphasize that these radiative forcings

apply to Mera La where impurity concentrations and glacier melt are greatest, whereas at higher elevations where impurity concentrations are lower, instantaneous radiative forcings would be less. Further in situ measurements from locations near the ELA of glaciers in the region are required to assess if the Mera La concentrations and instantaneous radiative forcings are representative of this elevation band on the south slope of the Himalaya.

These results suggest that the albedo and radiative forcing effect of dust is considerably greater than BC, even when considering the $_{\mathrm{M}}\mathrm{BC} \times 2$ and $_{\mathrm{M}}\mathrm{BC} \times 5$ scenarios. In this analysis the dust concentrations were inferred from the gravimetric mass, however we can further examine the relative absorption of BC vs. dust using the Fe concentrations. Iron oxides dominate light absorption by mineral dust, with 44–65 % of the Fe in the form of light-absorbing iron oxides (Lafon et al., 2004) that have a MAC of $0.56\,\mathrm{m^2\,g^{-1}}$ (Alfaro et al., 2004). Using the same MAC range for BC as used above, we calculated the absorption of BC vs. dust assuming that a range between 44–65 % of the Fe is light absorbing, and calculated the difference if the Fe was made up of hematite (Fe_2O_3) vs. goethite ($FeHO_2$). Lafon et al. (2006) reported that for Chinese dust, the fraction of iron oxides that is goethite and hematite are 73 and 27 %, respectively. We convert the Fe mass to hematite or goethite[1]:

$$\text{Hematite conversion factor}: ((56 \times 2) + (16 \times 3))/112 = 1.4,$$

$$\text{Goethite* conversion factor}: ((56 + 1 + (16 \times 2))/56 = 1.6,$$

and calculate the dust absorption by:

$$\mathrm{Fe_m} \times \mathrm{Fe_{abs}} \times C \times \mathrm{MAC} = \text{Dust Absorption } (\mathrm{m^2}),$$

where $\mathrm{Fe_m}$ is the Fe measured by ICP-MS in the snow/ice sample, $\mathrm{Fe_{abs}}$ is the fraction of the measured Fe that is light absorbing, C is the hematite or goethite conversion factor, and MAC is $0.56\,\mathrm{m^2\,g^{-1}}$ for iron oxides (Alfaro et al., 2004). The BC absorption is calculated by:

$$\mathrm{BC_m} \times \mathrm{MAC} = \text{BC Absorption } (\mathrm{m^2}),$$

where $\mathrm{BC_M}$ is the measured BC, and MAC ranges between 5.9 to $7.5\,\mathrm{m^2\,g^{-1}}$ as described above.

The following four scenarios were used to examine the relative absorption of dust vs. BC:

A. Dust most absorptive: assume iron oxide form as goethite, with 65 % of the iron as light absorbing, and a low MAC for BC ($5.9\,\mathrm{m^2\,g^{-1}}$ based on measured BC size distributions).

B. BC most absorptive: assume iron oxide form as hematite, with 44 % of the iron as light absorbing and high MAC for BC ($7.5\,\mathrm{m^2\,g^{-1}}$ based on commonly reported values).

C. BC most absorptive $\times$ 2: the same as in B, but in this case doubling the BC concentrations since $_{\mathrm{M}}\mathrm{BC}$ are underestimates.

D. BC most absorptive $\times$ 5: the same as in B, but in this case multiplying the BC concentrations by 5 since $_{\mathrm{M}}\mathrm{BC}$ are underestimates.

[1]Goethite is more absorptive when scaled to the ICP-MS Fe measurement because as hematite (Fe_2O_3) there are two iron atoms in one iron oxide molecule, whereas for goethite ($FeHO_2$) there is one Fe atom per iron oxide molecule.

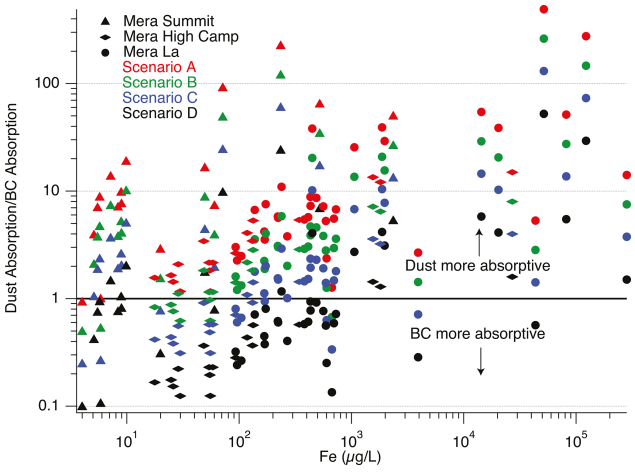

Figure 6. Fe concentrations vs. the calculated dust absorption/BC absorption for all snow samples presented in Fig. 4 of the manuscript based on the four scenarios described in the text.

Based on Scenario A, for all samples dust is more absorptive than BC, but how much more absorptive depends on the Fe concentration of the sample (Fig. 6). For samples with relatively low Fe concentrations ($< 50\,\mu\mathrm{g\,L^{-1}}$), dust is $\sim$1–11 $\times$ more absorptive than BC, whereas for samples with relatively high Fe concentrations, dust is estimated to be considerably more absorptive (maximum dust absorption/BC absorption = 490). For Scenarios B, C and D, whether dust or BC is more absorptive varies with Fe concentration. For samples with low Fe concentrations, BC is more absorptive, whereas for samples with higher Fe concentrations, dust is more absorptive than BC. Based on existing knowledge, these scenarios bracket the plausible range of dust absorption/BC absorption for the snow samples ($n = 70$) collected from Mera glacier. For samples with relatively high BC concentrations, the $\mathrm{BC_m} \times 2$ and $\mathrm{BC_m} \times 5$ scenarios are likely overestimates since in highly concentrated samples BC losses are less, but this detail becomes inconsequential because for samples with high BC and dust concentrations, the dust strongly dominates absorption.

We conducted similar analysis applying the MAC for Asian dust generically measured by Clarke et al. (2004) ($\mathrm{MAC} = 0.009\,\mathrm{m^2\,g^{-1}}$ at 550 nm) and Yang et al. (2009) ($\mathrm{MAC} = 0.037\,\mathrm{m^2\,g^{-1}}$ at 520 nm) to the gravimetric dust samples. Using a MAC for BC of $7.5\,\mathrm{m^2\,g^{-1}}$ and the

measured BC concentrations results in dust being 10–230 × more absorptive than BC based on the Clarke dust MAC and 40–937 × more absorptive based on the Yang dust MAC. If we multiply the BC concentrations × 5 to account for BC losses, dust is calculated to be 2–45 × more absorptive than BC based on the Clarke dust MAC and 8–187 × more absorptive based on the Yang dust MAC.

Our results suggest that when dust concentrations are high, dust dominates absorption, snow albedo reduction, and radiative forcing, and the impact of BC may be negligible. When impurity concentrations are low, the absorption by BC and dust may be comparable; however, due to the low concentrations, albedo reductions will be considerably less and radiative forcing minimal. Thus, dust deposition may dominate snow albedo in this region; however, there are several sources of uncertainty, including: (1) particle size that affects the assumed MAC for both dust and BC, (2) the amount of Fe or dust that is light absorbing, (3) the mixing state between BC, dust, and other constituents, and (4) how impurities accumulate at the glacier surface over the course of the year and how radiative forcing progresses. Considerably more work is needed to address the relative absorption of dust, BC, and colored organics. Ultimately, airborne and spaceborne imaging spectrometers and field-based spectrometry and in situ measurements will characterize the time variation of radiative forcing. New methods are needed to infer spectral complex refractive indices from bulk samples and to partition them into BC, dust, and organics.

3.4 Implications for Himalayan glaciers, snowmelt, and radiative forcing

Glaciers in the eastern Himalaya are summer accumulation type glaciers. During summer, substantial precipitation falls associated with the South Asian monsoon, and ablation is also at a maximum (Ageta and Higuchi, 1984). If the high impurity layers that form during the winter–spring period are covered by fresh snowfall during the summer season, the effect of BC and dust on summer glacier melt would be largely eliminated. Conversely, if the impurities are exposed at the glacier surface during the melt season, glacier melt would be accelerated. This could occur if melt results in the re-exposure of impurities at the glacier surface, and/or if the melt season is expanded due to a warming climate (Fujita, 2007; Fujita et al., 2011; Yasunari et al., 2010). The spatial distribution of precipitation in this region is largely unknown. However, remote sensing of the Himalaya suggests that for elevations < 7000 m, the snow covered area does not increase during summer (Maskey et al., 2011) and therefore these impurities should remain exposed, whereas at higher elevations summer snowfall would diminish the impacts of winter/spring accumulation of BC and dust.

While this study documents substantial BC and dust at 5400 m to result in a reduction of the glacier albedo, it isn't clear if sufficient light-absorbing impurities are present at higher elevations for a notable reduction in albedo to occur. The maximum $_{M}$BC in the snow pits sampled at Mera Col at 6400 m a.s.l. in this study was 8.4 µg L^{-1}, and the shallow Mera Peak ice core from 6376 m a.s.l. had maximum and mean BC of 47.9 and 3 µg L^{-1}, respectively (Ginot et al., 2013). $_{M}$BC concentrations in an ice core collected from the col of the nearby East Rongbuk glacier (6518 m a.s.l.) on the northeast side of Mt. Everest and analyzed for BC by the same methods employed in this study were comparable to BC concentrations at Mera Col, with lower $_{M}$BC concentrations than the lower Mera elevation sites (Table 1; Kaspari et al., 2011). Relatively low $_{M}$BC concentrations on East Rongbuk and Mera glaciers at ∼ 6400 m suggests that, at least over short distances, a strong gradient in BC deposition does not exist between the southern and northern slopes of the Himalaya. As stated before, $_{M}$BC reported herein represent lower-limit BC values, so our results are not conclusive regarding the contribution of BC to albedo reduction on glaciers and seasonal snow at elevations greater than 6000 m a.s.l. Our results do, however, suggest that BC contributes to a greater albedo reduction at elevations below ∼ 6000 m a.s.l., but when in the presence of large dust concentrations, BC contributes little forcing.

To assess potential impacts of BC and dust on snow and ice, variations in the amount of snow and ice with elevation needs to be considered. In the Nepalese Himalaya at elevations greater than 6000 m, the fraction of land that is snow covered is in excess of 60 % throughout the year, whereas for elevations lower than 6000 m with the exception of February–March, it is less than 40 % (Maskey et al., 2011). Assuming that the elevation gradient in BC and dust concentrations observed in this study also exists on other glaciers in the region, it can be inferred that in the regions with the greatest fraction of snow-covered land, BC and dust concentrations are relatively low. However, for land area above 3000 m in the Nepalese Himalaya, the fraction at elevations greater than 6000 m is less than 1 %, whereas 90 % of the land lies in the elevation zone between 4000 and 6000 m (Maskey et al., 2011). Thus, the largest areal extent of snow-covered area lies in the 4000 to 6000 m zone, where BC and dust concentrations in snow and ice were observed to be highest.

That BC and dust-induced albedo reduction and the concentrations of snow and ice varies with elevation has implications for glacial mass balance, water resources, and radiative forcing. At elevations above ∼ 6000 m lie the accumulation zones of glaciers, and a large fraction of the land area is snow covered. However, the small fraction of land at elevations greater than 6000 m combined with minimal surface melt and relatively low BC and dust concentrations suggest that light-absorbing impurities in the high Himalaya do not affect water resources and radiative forcing to the degree that is likely at lower elevations. While our results are described

in a binary fashion due to sampling logistics, the impact of BC and dust on glacier melt and water resources occurs in a continuous convolution of surface concentrations, spatial extent, snow water equivalent, and energy fluxes. At higher elevations, concentrations are lower, area is smaller, and energy fluxes are smaller in composite, while snow water equivalent (SWE) is relatively high. Nevertheless, BC and dust anomalies, however small, increase net solar radiation and warm the snowpack. At lower snow-covered elevations, concentrations are higher, spatial extent is larger, and energy fluxes are generally larger. The greatest impact on glacier melt comes from the rising of the equilibrium line altitude (ELA) from earlier removal of snow cover, and glacier ice then being subject to markedly greater energy fluxes.

BC and dust have the potential to accelerate glacial and seasonal snowmelt, which could impact water resources if the timing and magnitude of runoff is altered. Using a numerical model applied to BC observed on a Tibetan glacier, Yasunari et al. (2010) estimated that a 2.0–5.2 % albedo reduction from BC deposition could result in a 11.6–33.9 % increase in annual discharge if the reduced albedo snow layer remained at the glacier surface. While this increase in discharge likely overestimates actual increases in discharge since snow with a lower BC concentration and higher albedo is deposited during the summer monsoon, it nevertheless highlights that BC has the potential to accelerate snow/ice melt. However, our findings suggest that in the presence of high dust concentrations, the efficacy of BC to induce melt is lessened. Thus, further research is needed to partition light-absorbing impurities into their various components (BC, dust, organics) along with a more holistic treatment of light-absorbing impurity-induced melt. This is particularly important in the context of determining the degree to which snow and glacier melt is being driven by increased deposition of light-absorbing impurities from anthropogenic activities. Since a substantial portion of dust originates from natural sources, partitioning the contribution of BC and dust deposition from anthropogenic as opposed to natural sources is challenging.

4 Conclusions

This study provides the first observational data of BC and dust concentrations from the southern slope of the Himalaya. A strong elevation gradient is observed, with BC and dust concentrations substantially higher at elevations < 6000 m than > 6000 m due to post-depositional processes including melt and sublimation, and likely greater deposition at lower elevations. This elevation gradient has important implications for spatial variations in impurity deposition, radiative forcing, and melt. Because the largest areal extent of snow and ice resides at elevations < 6000 m, the higher BC and dust concentrations at these elevations can reduce the snow and glacier albedo over large areas, accelerating melt, affecting glacier mass balance and water resources, and contributing to a positive climate forcing.

Radiative transfer modeling and calculations of the relative absorption of dust vs. BC constrained by the observational data indicate that the snow albedo and radiative forcing of dust is considerably greater than BC. When dust concentrations are high, dust dominates absorption, snow albedo reduction, and radiative forcing, and the impact of BC may be negligible. When impurity concentrations are low, the absorption by BC and dust may be comparable; however, due to the low concentrations albedo reductions will be considerably less. However, there are several sources of uncertainty, including particle size; the amount of dust that is light absorbing; the mixing state between BC, dust and other constituents; and the presence of other light-absorbing impurities including colored organics, humic-like substances, snow algae, and bacteria. Further observational studies are needed to assess the relative contribution of different absorbing impurities to albedo reductions and snow and ice melt, including the temporal evolution of how impurities accumulate and radiative forcing progresses throughout the year. If further investigation confirms that dust is the dominant light-absorbing impurity, the amount of dust originating from natural vs. anthropogenic sources will require further attention. Lastly, in addition to light-absorbing impurities, there are several other factors that also contribute to changes in the cryosphere in the Himalaya include higher air temperatures (Yang et al., 2011), changes in snow accumulation (Kaspari et al., 2008), and variations in glacier velocities (Quincey et al., 2009).

Acknowledgements. We thank T. D. Sherpa, J. Cunningham, and the Nepali staff for assistance in the field during the spring 2009 field season; Y. Arnaud and P. Wagnon for collecting the fall 2009 snow samples and for valuable information about the Mera region; EV-K2-CNR for collection of fresh snow samples at NCO-P and assistance with obtaining permits; and Y. Balkanski and three anonymous reviewers for their suggestions that improved the manuscript. W. Szeliga calculated the BC MAC value based on measured BC size distributions and Sarah Doherty and Dean Hegg provided helpful insight on using Fe to constrain dust absorption. This research was funded by the National Science Foundation (OISE-0653933 and EAR-0957935), NASA project NNX10AO97G, and partially supported by the Office of the Dean, College of the Sciences, Central Washington University, Ellensburg, Washington. Collection of fresh snow samples at NCO-P was carried out within the framework of the EV-K2-CNR project in collaboration with the Nepal Academy of Science and Technology as foreseen by the Memorandum of Understanding between Nepal and Italy, and thanks to contributions from the Italian National Research Council. M. Gysel received financial support from the Swiss National Science Foundation.

Edited by: Y. Balkanski

References

Ageta, Y. and Higuchi, K.: Estimation of mass balance components of a summer-accumulation type glacier in the Nepal Himalaya, Geogr. Ann. A, 66, 249–255, 1984.

Alfaro, S. C., Lafon, S., Rajot, J. L. , Formenti, P., Gaudichet, A., and Maille, M., Iron oxides and light absorption by pure desert dust: An experimental study, J. Geophys. Res., 109, D08208, doi:10.1029/2003JD004374, 2004.

Andreae, M. O. and Gelencsér, A.: Black carbon or brown carbon? The nature of light-absorbing carbonaceous aerosols, Atmos. Chem. Phys., 6, 3131–3148, doi:10.5194/acp-6-3131-2006, 2006.

Barnett, T. P., Adam, J. C., and Lettenmaier, D. P.: Potential impacts of a warming climate on water availability in snow-dominated regions, Nature, 438, 303–309, doi:10.1038/nature04141, 2005.

Bolch, T., Kulkarni, A., Kääb, A., Huggel, C., Paul, F., Cogley, J. G., Frey, H., Kargel, J. S., Fujita, K., Scheel, M., Bajracharya, S., and Stoffel, M.: The State and Fate of Himalayan Glaciers, Science, 336, 310–314, 2012.

Bonasoni, P., Laj, P., Marinoni, A., Sprenger, M., Angelini, F., Arduini, J., Bonafè, U., Calzolari, F., Colombo, T., Decesari, S., Di Biagio, C., di Sarra, A. G., Evangelisti, F., Duchi, R., Facchini, MC., Fuzzi, S., Gobbi, G. P., Maione, M., Panday, A., Roccato, F., Sellegri, K., Venzac, H., Verza, GP., Villani, P., Vuillermoz, E., and Cristofanelli, P.: Atmospheric Brown Clouds in the Himalayas: first two years of continuous observations at the Nepal Climate Observatory-Pyramid (5079 m), Atmos. Chem. Phys., 10, 7515–7531, doi:10.5194/acp-10-7515-2010, 2010.

Bond, T. and Bergstrom, R.: Light Absorption by Carbonaceous Particles: An Investigative Review, Aerosol Sci. Tech., 40, 27–67, 2006.

Bond, T., Bhardwaj, E., Dong, R., Jogani, R., Jung, S., Roden, C., Streets, D. G., and Trautmann, N.: Historical emissions of black and organic carbon aerosol from energy-related combustion, 1850–2000, Global Biogeochem. Cy., 21, GB2018, doi:10.1029/2006GB002840, 2007.

Bond, T. C., Streets, D. G., Yarber, K. F., Nelson, S. M., Woo, J.-H., and Klimont, Z.: A technology-based global inventory of black and organic carbon emissions from combustion, J. Geophys. Res., 109, D14203, doi:10.1029/2003JD003697, 2004.

Bond, T. C., Doherty, S. J., Fahey, D. W., Forster, P. M., Berntsen, T., DeAngelo, B. J., Flanner, M. G., Ghan, S., Kärcher, B., Koch, D., Kinne, S., Kondo, Y., Quinn, P. K., Sarofim, M. C., Schultz, M. G., Schulz, M., Venkataraman, C., Zhang, H., Zhang, S., Bellouin, N., Guttikunda, S. K., Hopke, P. K., Jacobson, M. Z., Kaiser, J. W., Klimont, Z., Lohmann, U., Schwarz, J. P., Shindell, D., Storelvmo, T., Warren, S. G., and Zender, C. S.: Bounding the role of black carbon in the climate system: A scientific assessment, J. Geophys. Res.-Atmos., 118, 5380–5552, doi:10.1002/jgrd.50171, 2013.

Brandt, R. E., Warren, S. G., and Clarke, A. D.: A controlled snowmaking experiment testing the relation between black carbon content and reduction of snow albedo, J. Geophys. Res.-Atmos., 116, D08109, doi:10.1029/2010jd015330, 2011.

Chang, H. and Charalampopoulos, T. T.: Determination of the wavelength dependence of refractive indices of flame soot, Proceedings: Mathematical and Physical Sciences, 430, 577–591, 1990.

Clarke, A. D., Shinozuka, Y., Kapustin, V. N., Howell, S., Huebert, B., Doherty, S., Anderson, T., Covert, D., Anderson, J., Hua, X., Moore II, K. G., McNaughton, C., Carmichael, G., and Weber, R.: Size distributions and mixtures of dust and black carbon aerosol in Asian outflow: Physiochemistry and optical properties, J. Geophys. Res., 109, D15S09, doi:10.1029/2003JD004378, 2004.

Cong, Z., Kang, S., and Qin, D.: Seasonal features of aerosol particles recorded in snow from Mt. Qomolangma (Everest) and their environmental implications, J. Environ. Sci., 21, 914–919, 2009.

Conway, H., Gades, A., and Raymond, C. F.: Albedo of dirty snow during conditions of melt, Water Resour. Res., 32, 1713–1718, 1996.

Flanner, M. G. and Zender, C. S.: Linking snowpack microphysics and albedo evolution, J. Geophys. Res.-Atmos., 111, D12208, doi:10.1029/2005jd006834, 2006.

Flanner, M. G., Zender, C. S., Randerson, J. T., and Rasch, P. J.: Present-day climate forcing and response from black carbon in snow, J. Geophys. Res., 112, D11202, doi:10.1029/2006JD008003, 2007.

Flanner, M. G., Zender, C. S., Hess, P. G., Mahowald, N. M., Painter, T. H., Ramanathan, V., and Rasch, P. J.: Springtime warming and reduced snow cover from carbonaceous particles, Atmos. Chem. Phys., 9, 2481–2497, doi:10.5194/acp-9-2481-2009, 2009.

Fujita, K.: Effect of dust event timing on glacier runoff: sensitivity analysis for a Tibetan glacier, Hydrol. Process., 21, 2892–2896, doi:10.1002/hyp.6504, 2007.

Fujita, K., Takeuchi, N., Nikitin, S. A., Surazakov, A. B., Okamoto, S., Aizen, V. B., and Kubota, J.: Favorable climatic regime for maintaining the present-day geometry of the Gregoriev Glacier, Inner Tien Shan, The Cryosphere, 5, 539–549, doi:10.5194/tc-5-539-2011, 2011.

Gautam, R., Hsu, N. C., Lau, W. K. M., and Yasunari, T. J.: Satellite observations of desert dust-induced Himalayan snow darkening, Geophys. Res. Lett., 40, 988–993, doi:10.1002/grl.50226, 2013.

Ginot, P., Dumont, M., Lim, S., Patris, N., Taupin, J.-D., Wagnon, P., Gilbert, A., Arnaud, Y., Marinoni, A., Bonasoni, P., and Laj, P.: A 10 yr record of black carbon and dust from Mera Peak ice core (Nepal): variability and potential impact on Himalayan glacier melting, The Cryosphere Discuss., 7, 6001–6042, doi:10.5194/tcd-7-6001-2013, 2013.

Grenfell, T. C., Perovich, D. K., and Ogren, J. A.: Spectral albedos of an alpine snowpack, Cold Reg. Sci. Technol., 4, 121–127, 1981.

Grenfell, T. C., Warren, S., and Mullen, P. C.: Reflection of solar radiation by the Antarctic snow surface at ultraviolet, visible,and near-infrared wavelengths, J. Geophys. Res., 99, 18669–18684, 1994.

Hadley, O. L. and Kirchstetter, T. W.: Black carbon reduction of snow albedo, Nature Clim. Change, 2, 437–440, 2012.

Hansen, J. and Nazarenko, L.: Soot climate forcing via snow and ice albedos, P. Natl. Acad. Sci. USA, 101, 423–428, 2004.

Immerzeel, W. W., van Beek, L. P. H., and Bierkens, M. F. P.: Climate Change Will Affect the Asian Water Towers, Science, 328, 1382–1385, doi:10.1126/science.1183188, 2010.

Jacobson, M. Z.: Climate response of fossil fuel and biofuel soot, accounting for soot's feedback to snow and sea

ice albedo and emissivity, J. Geophys. Res., 109, D21201, doi:10.1029/2004JD004945, 2004.

Kaspari, S., Hooke, R., Mayewski, P. A., Kang, S., Hou, S., and Qin, D.: Snow accumulation rate on Qomolangma (Mt. Everest): synchroneity with sites across the Tibetan Plateau on 50-100 year timescales, J. Glaciol., 54, 343–352, 2008.

Kaspari, S., Mayewski, P. A., Handley, M. J., Kang, S., Hou, S., Maasch, K., and Qin, D.: A High-Resolution Record of Atmospheric Dust Composition and Variability since a.d. 1650 from a Mount Everest Ice Core, J. Climate, 22, 3910–3925, doi:10.1175/2009JCLI2518.1, 2009.

Kaspari, S., Schwikowski, M., Gysel, M., Flanner, M. G., Kang, S., Hou, S., and Mayewski, P. A.: Recent increase in black carbon concentrations from a Mt. Everest ice core spanning 1860–2000 AD, Geophys. Res. Lett., 38, L04703, doi:10.1029/2010GL046096, 2011.

Kopacz, M., Mauzerall, D. L., Wang, J., Leibensperger, E. M., Henze, D. K., and Singh, K.: Origin and radiative forcing of black carbon transported to the Himalayas and Tibetan Plateau, Atmos. Chem. Phys., 11, 2837–2852, doi:10.5194/acp-11-2837-2011, 2011.

Lafon, S., Rajot, J. L., Alfaro, S., and Gaudichet, A.: Quantification of iron oxides in desert aerosol, Atmos. Environ., 38, 1211–1218, 2004.

Lafon, S., Sokolik, I. N., Rajot, J. L., Caquineau, S., and Gaudichet, A.: Characterization of iron oxides in mineral dust aerosols: Implications for light absorption, J. Geophys. Res., 111, D21207, doi:10.1029/2005JD007016, 2006.

Lawrence, C. R., Painter, T. H., Landry, C. C., and Neff, J. C., Contemporary geochemical composition and flux of aeolian dust to the San Juan Mountains, Colorado, United States, J. Geophys. Res., 115, G03007, doi:10.1029/2009JG001077, 2010.

Lim, S., Faïn, X., Zanatta, M., Cozic, J., Jaffrezo, J.-L., Ginot, P., and Laj, P.: Refractory black carbon mass concentrations in snow and ice: method evaluation and inter-comparison with elemental carbon measurement, Atmos. Meas. Tech. Discuss., 7, 3549–3589, doi:10.5194/amtd-7-3549-2014, 2014.

Liu, X., Xu, B., Yao, T., Wang, N., and Wu, G.: Carbonaceous particles in Muztag Ata ice core, West Kunlun Mountains, China, Chinese Sci. Bull., 53, 3379–3386, 2008.

Marinoni, A., Cristofanelli, P., Laj, P., Duchi, R., Calzolari, F., Decesari, S., Sellegri, K., Vuillermoz, E., Verza, G. P., Villani, P., and Bonasoni, P.: Aerosol mass and black carbon concentrations, a two year record at NCO-P (5079 m, Southern Himalayas), Atmos. Chem. Phys., 10, 8551–8562, doi:10.5194/acp-10-8551-2010, 2010.

Maskey, S., Uhlenbrook, S., and Ojha, S.: An analysis of snow cover changes in the Himalayan region using MODIS snow products and in-situ temperature data, Clim. Change, 108, 391–400, doi:10.1007/s10584-011-0181-y, 2011.

Ming, J., Cachier, H., Xiao, C., Qin, D., Kang, S., Hou, S., and Xu, J.: Black carbon record based on a shallow Himalayan ice core and its climatic implications, Atmos. Chem. Phys., 8, 1343–1352, doi:10.5194/acp-8-1343-2008, 2008.

Ming, J., Xiao, C., Cachier, H., Qin, D., Qin, X., Li, Z., and Pu, J.: Black Carbon (BC) in the snow of glaciers in west China and its potential effects on albedos, Atmos. Res., 92, 114–123, 2009.

Ming, J., Du, Z., Xiao, C., Xu, X., and Zhang, D.: Darkening of the mid-Himalaya glaciers since 2000 and the potential causes, Environ. Res. Lett., 7, 014021, doi:10.1088/1748-9326/7/1/014021, 2012.

Painter, T., Barrett, A. P., Landry, C. C., Neff, J. C., Cassidy, M. P., Lawrence, C. R., McBride, K. E., and Farmer, G. L.: Impact of disturbed desert soils on duration of mountain snow cover, Geophys. Res. Lett., 34, L12502, doi:10.1029/2007GL030284, 2007.

Painter, T. H.: Comment on Singh and others, "Hyperspectral analysis of snow reflectance to understand the effects of contamination and grain size", J. Glaciol., 57, 183–185, 2011.

Painter, T. H., Skiles, S. M., Deems, J. S., Bryant, A. C., and Landry, C. C.: Dust radiative forcing in snow of the Upper Colorado River Basin: 1. A 6 year record of energy balance, radiation, and dust concentrations, Water Resour. Res., 48, W07521, doi:10.1029/2012WR011985, 2012.

Painter, T. H., Seidel, F., Bryant, A. C., Skiles, S. M., and Rittger, K.: Imaging spectroscopy of albedo and radiative forcing by light-absorbing impurities in mountain snow, J. Geophys. Res. Atmos., 118, 9511–9523, doi:10.1002/jgrd.50520, 2013.

Petzold, A., Ogren, J. A., Fiebig, M., Laj, P., Li, S.-M., Baltensperger, U., Holzer-Popp, T., Kinne, S., Pappalardo, G., Sugimoto, N., Wehrli, C., Wiedensohler, A., and Zhang, X.-Y.: Recommendations for reporting "black carbon" measurements, Atmos. Chem. Phys., 13, 8365–8379, doi:10.5194/acp-13-8365-2013, 2013.

Quincey, D. J., Luckman, A., and Benn, D.: Quantification of Everest region glacier velocities between 1992 and 2002, using satellite radar interferometry and feature tracking, J. Glaciol., 55, 596–606, 2009.

Ramanathan, V. and Carmichael, G. R.: Global and regional climate changes due to black carbon, Nat. Geosci., 1, 221–227, 2008.

Ricchiazzi, P., Yang, S. R., Gautier, C., and Sowle, D.: SBDART: A research and teaching software tool for plane-parallel radiative transfer in the Earth's atmosphere, B. Am. Meteorol. Soc., 79, 2101–2114, 1998.

Schwarz, J. P., Gao, R. S., Fahey, D. W., Thomson, D. S., Watts, L. A., Wilson, J. C., Reeves, J. M., Darbeheshti, M., Baumgardner, D. G., Kok, G. L., Chung, S. H., Schulz, M., Hendricks, J., Lauer, A., Kärcher, B., Slowik, J. G., Rosenlof, K. H., Thompson, T. L., Langford, A. O., Loewenstein, M., and Aikin, K. C.: Single-particle measurements of midlatitude black carbon and light-scattering aerosols from the boundary layer to the lower stratosphere, J. Geophys. Res., 111, D16207, doi:10.1029/2006JD007076, 2006.

Schwarz, J. P., Doherty, S. J., Li, F., Ruggiero, S. T., Tanner, C. E., Perring, A. E., Gao, R. S., and Fahey, D. W.: Assessing Single Particle Soot Photometer and Integrating Sphere/Integrating Sandwich Spectrophotometer measurement techniques for quantifying black carbon concentration in snow, Atmos. Meas. Tech., 5, 2581–2592, doi:10.5194/amt-5-2581-2012, 2012.

Schwarz, J. P., Gao, R. S., Perring, A. E., Spackman, J. R., and Fahey, D. W.: Black carbon aerosol size in snow, Nat. Sci. Reports, 3, 1356, doi:10.1038/srep01356, 2013.

Singh, S. K., Kulkarni, A., and Chaudhary, B. S.: Hyperspectral analysis of snow reflectance to understand the effects of contamination and grain size, Ann. Glaciol., 51, 83–88, 2010.

Slowik, J. G., Cross, E. S., Han, J., Davidovits, P., Onasch, T. B., Jayne, J. T., Williams, L. R., Canagaratna, M. R., Worsnop, D. R., Chakrabarty, R. K., Moosmüller, H., Arnott, W. P., Schwarz,

J. P., Gao, R. S., Fahey, D. W., Kok, G. L., and Petzold, A.: An inter-comparison of instruments measuring black carbon content of soot particles, Aerosol Sci. Tech., 41, 295–314, 2007.

Stephens, M., Turner, N., and Sandberg, J.: Particle identification by laser-induced incandescence in a solid-state laser cavity, Appl. Optics, 42, 3726–3736, 2003.

Takeuchi, N.: Optical characteristics of cryoconite (surface dust) on glaciers: the relationship between light absorbency and the property of organic matter contained in the cryoconite, Ann. Glaciol., 34, 409–414, 2002.

Thompson, L. G., Yao, T., Mosley-Thompson E., Davis, M., Henderson, B., and Lin, P. N.: A high-resolution millennial record of the South Asian Monsoon from Himalayan ice cores, Science, 289, 1916–1919, 2000.

Torres, A., Bond, T. C., Lehmann, C. M. B., Subramanian, R., and Hadley, O.: Measuring Organic Carbon and Black Carbon in Rainwater: Evaluation of Methods, Aerosol Sci. Tech., 48, 3, 239–350, 2014.

Venkataraman, C., Habib, G., Eiguren-Fernandez, A., Miguel, A. H., and Friedlander, S. K.: Residential biofuels in south Asia: Carbonaceous aerosol emissions and climate impacts, Science, 307, 1454–1456, doi:10.1126/science.1104359, 2005.

Venkataraman, C., Habib, G., Kadamba, D., Shrivastava, M., Leon, J.-F., Crouzille, B., Boucher, O., and Streets, D. G.: Emissions from open biomass burning in India: Integrating the inventory approach with high-resolution Moderate Resolution Imaging Spectroradiometer (MODIS) active-fire and land cover data, Global Biogeochem. Cy., 20, GB2013, doi:10.1029/2005GB002547, 2006.

Wagnon, P., Vincent, C., Arnaud, Y., Berthier, E., Vuillermoz, E., Gruber, S., Ménégoz, M., Gilbert, A., Dumont, M., Shea, J. M., Stumm, D., and Pokhrel, B. K.: Seasonal and annual mass balances of Mera and Pokalde glaciers (Nepal Himalaya) since 2007, The Cryosphere, 7, 1769–1786, doi:10.5194/tc-7-1769-2013, 2013.

Warren, S. and Wiscombe, W.: A model for the spectral albedo of snow II. Snow containing atmospheric aerosols, J. Atmos. Sci., 37, 2734–2745, 1980.

Warren, S. and Wiscombe, W.: Dirty snow after nuclear war, Nature, 313, 467–470, doi:10.1038/313467a0, 1985.

Wedepohl, K. H.: The composition of the continental crust, Geochim. Cosmochim. Ac., 59, 1217–1232, 1995.

Wendl, I. A., Menking, J. A., Färber, R., Gysel, M., Kaspari, S. D., Laborde, M. J. G., and Schwikowski, M.: Optimized method for black carbon analysis in ice and snow using the Single Particle Soot Photometer, Atmos. Meas. Tech. Discuss., 7, 3075–3111, doi:10.5194/amtd-7-3075-2014, 2014.

Wiscombe, W. and Warren, S.: A model for the spectral albedo of snow. I: Pure Snow, J. Atmos. Sci., 37, 2712–2733, 1980.

Xu, B., Cao, J., Hansen, J., Yao, T., Joswiak, D., Wang, N., Wu, G., Wang, M., Zhao, H., Yang, W., Liu, X., and He, J.: Black soot and the survival of Tibetan glaciers, P. Natl. Acad. Sci. USA, 106, 22114–22118, 2009.

Xu, B., Cao, J., Joswiak, D., Liu, X., Zhao, H., and He, J.: Post-depositional enrichment of black soot in snow-pack and accelerated melting of Tibetan glaciers, Environ. Res. Lett., 7, 014022, doi:10.1088/1748-9326/7/1/014022, 2012.

Yang, M., Howell, S. G., Zhuang, J., and Huebert, B. J.: Attribution of aerosol light absorption to black carbon, brown carbon, and dust in China – interpretations of atmospheric measurements during EAST-AIRE, Atmos. Chem. Phys., 9, 2035–2050, doi:10.5194/acp-9-2035-2009, 2009.

Yang, X. G., Zhang, T. J., Qin, D. H., Kang, S. C., and Qin, X. A.: Characteristics and Changes in Air Temperature and Glacier's Response on the North Slope of Mt. Qomolangma (Mt. Everest), Arct. Antarct. Alp. Res., 43, 147–160, doi:10.1657/1938-4246-43.1.147, 2011.

Yasunari, T. J., Bonasoni, P., Laj, P., Fujita, K., Vuillermoz, E., Marinoni, A., Cristofanelli, P., Duchi, R., Tartari, G., and Lau, K.-M.: Estimated impact of black carbon deposition during pre-monsoon season from Nepal Climate Observatory – Pyramid data and snow albedo changes over Himalayan glaciers, Atmos. Chem. Phys., 10, 6603–6615, doi:10.5194/acp-10-6603-2010, 2010.